Savoie, R., Boulé, B., Genest, G., & Pézolet, M. (1979) *Can. J. Spectrosc. 24*, 112-117.
Silvius, J. R., & Gagné, J. (1984a) *Biochemistry 23*, 3232-3240.
Silvius, J. R., & Gagné, J. (1984b) *Biochemistry 23*, 3241-3247.
Snyder, R. G., & Scherer, J. R. (1979) *J. Chem. Phys. 71*, 3221-3228.
Snyder, R. G., Hsu, S. L., & Krimm, S. (1978) *Spectrochim. Acta, Part A 34A*, 395-406.
Snyder, R. G., Scherer, J. R., & Gaber, B. P. (1980) *Biochim. Biophys. Acta 601*, 47-53.
Spiker, R. C., Jr., & Levin, I. W. (1975) *Biochim. Biophys. Acta 338*, 361-373.
Susi, H. (1981) *Chem. Phys. Lipids 29*, 359-368.
Van Dick, P. W. M., de Kruijff, B., Verkleij, A. J., Van Deenen, L. L. M., & de Gier, J. (1978) *Biochim. Biophys. Acta 512*, 84-96.
Verkleij, A. J., de Kruijff, B., Ververgaert, P. H. J. Th., Tocanne, J. F., & Van Deenen, L. L. M. (1974) *Biochim. Biophys. Acta 339*, 432-437.
Verkleij, A. J., de Maagd, R., Leunissen-Bijvelt, J., & de Kruijff, B. (1982) *Biochim. Biophys. Acta 684*, 255-262.

Flexibility of the Molecular Forms of Acetylcholinesterase Measured with Steady-State and Time-Correlated Fluorescence Polarization Spectroscopy†

Harvey Alan Berman,*,‡ Juan Yguerabide,§ and Palmer Taylor‡

Division of Pharmacology, Department of Medicine, and Department of Biology, University of California, San Diego, La Jolla, California 92093

Received October 4, 1984

ABSTRACT: Steady-state and time-correlated fluorescence polarizations have been examined for selected complexes and covalent conjugates of the 11S and (17 + 13)S forms of *Torpedo* acetylcholinesterase. The 11S form exists as a tetramer of apparently identical subunits, whereas the (17 + 13)S forms contain two or three sets of tetramers disulfide-linked to an elongated collagen-like tail unit. Pyrenebutyl methylphosphonofluoridate and (dansylsulfonamido)pentyl methylphosphonofluoridate were conjugated at the active center serine whereas propidium was employed as a fluorescent ligand for the spatially removed peripheral anionic site. Steady-state polarization of the pyrenebutyl conjugates indicates rotational correlation times of approximately 400 ns for the 11S species and greater than 1100 ns for the (17 + 13)S species. Hence, the tail unit severely restricts rotational motion of the catalytic subunits. Time-correlated fluorescence polarization analysis of the 11S species indicates multiple rotational correlation times. Anisotropy decay of the propidium complex (τ = 6 ns) occurs in exponential manner with a rotational correlation time of $\sim$150 ns, while covalent adducts at the active center exhibit rotational correlation times $\geq$300 ns. Anisotropy decay of the (dansylsulfonamido)pentyl conjugate (τ = 16 ns) appears exponential with a correlation time of approximately 320 ns, whereas decay of the pyrenebutyl conjugate (τ = 100 ns) is described by two correlation times, ϕ_S = 18 ns and ϕ_L = 320 ns, of small (15%) and large (85%) amplitudes, respectively. Two limiting models have been considered to explain the results. The first model considers the 11S form to behave as a *rigid* ellipsoid of revolution, whereas the second model incorporates the capacity for *segmental motion*. The biphasic decay seen with the longer lived probe and the differences in anisotropy decay seen for propidium and the active site ligands support the second model which incorporates protein flexibility.

Acetylcholinesterase (AchE)[1] can be isolated from electric organs of *Torpedo* as distinct molecular forms differing in molecular weight and complexity of structure (Lwebuga-Mukasa et al., 1976; Reiger et al., 1976; Viratelle & Bernhard, 1980; Bon & Massoulié, 1980; Lee et al., 1982a,b; Lee & Taylor, 1982). The 13S and 17S forms exist as large assemblies comprising two and three tetramers of catalytic subunits of 70000 daltons covalently associated through disulfide linkages with a collagenase-sensitive, filamentous tail unit and a noncollagenous subunit. The tail unit can be detected in electron micrographs as an elongated entity of 20 Å in diameter and 500 Å in length. Light tryptic digestion removes the noncollagenous and collagenous structural subunits, yielding an 11S species. The 11S or "lytic" form of acetylcholinesterase can be isolated as a tetrameric assembly comprised of four apparently equivalent subunits of 70000 daltons. As deduced from its frictional coefficient of 1.65, the 11S AchE species exhibits substantial dimensional asymmetry (Taylor et al., 1974). The catalytic subunits on the 11S and the tail-con-

† Supported by USPHS Grant GM-18360 to P.T., USPHS Grant ES-03085, and a grant from the U.S. Army Research Office to H.A.B.

* Address correspondence to this author at the Department of Biochemical Pharmacology, School of Pharmacy, State University of New York at Buffalo, Buffalo, NY 14260.
‡ Division of Pharmacology, Department of Medicine.
§ Department of Biology.

[1] Abbreviations: AchE, acetylcholinesterase; PBMP-AchE, (pyrenebutyl methylphosphono)acetylcholinesterase; DC_5MP-AchE, [(dansylsulfonamido)pentyl methylphosphono]acetylcholinesterase; PBMPF, pyrenebutyl methylphosphonofluoridate; Tris-HCl, tris(hydroxymethyl)aminomethane hydrochloride.

0006-2960/85/0424-7140$01.50/0

taining (17 + 13)S species appear to be structurally and catalytically equivalent (Lee et al., 1982a).

In addition to inhibition through direct association at the active center, a variety of inorganic cations and quaternary nitrogen-containing ligands alter the catalytic activity of AchE by association at a peripheral anionic site (Taylor & Lappi, 1975; Mooser & Sigman, 1974; Pattison & Bernhard, 1977; Epstein et al., 1979) situated a considerable distance from the active center (Berman et al., 1980). Such allosteric inhibition originating from ligand binding to physically remote sites might be expected to require the capacity for AchE to readily undergo changes in conformation, reflecting a corresponding flexibility in the subunits. To examine molecular motion in the AchE molecules, we have examined its rotational diffusion behavior employing steady-state and time-correlated nanosecond fluorescence spectroscopy. This technique monitors rotational Brownian motion of the emission transition moment and, in theory, provides information on the size, shape, and segmental motions of macromolecules (Yguerabide et al., 1970). Such methods yield the least ambiguous interpretations when fluorescence probes that bind at specific sites and in known stoichiometries are employed.

In this study, we describe measurements of anisotropy decay rates for two fluorescent phosphonates covalently conjugated at the active center serine of AchE and a reversible inhibitor of high affinity, propidium, specific for the peripheral anionic site. The fluorescent conjugates reveal different molecular motions of the various AchE species and enable an estimate of segmental motion in the 11S species.

Experimental Procedures

AchE from *Torpedo californica* was extracted to yield the lytic (11S) species by light trypsin digestion of membranes from the electric organ and purified to homogeneity by affinity chromatography on Sepharose 4B linked through an extended arm to (*m*-aminophenyl)trimethylammonium (Taylor et al., 1974). The capacity of propidium to intercalate into residual nucleic acid fragments necessitated an additional treatment of the purified protein with a micrococcal nuclease (from *Staphylococcus aureus*, Sigma) followed by a second sequence of adsorption and elution from the same affinity resin (Taylor & Lappi, 1975). The elongated forms were purified by affinity chromatography from high ionic strength extracts of a crude membrane fraction from *Torpedo* electric organs. In this case, aminoacridinium was linked through aminocaproic acid to Sepharose CL-4B (Lee et al., 1982a). Since residual quantities of 5.6S AchE are often present in this preparation, the material from the affinity column was concentrated and placed on a Sephacryl column equilibrated with 1 M NaCl, 0.04 M $MgCl_2$, and 0.01 M Tris-HCl, pH 8.0, containing 0.1% Triton X-100. The nonionic detergent was necessary to dissociate 5.6S species. After fractionation, Triton X-100 was removed with sequential treatments of Extractigel D (Pierce) and Amberlite [cf. Lee & Taylor (1982)]. The distribution of elongated species was ascertained from density gradient centrifugation and appeared in the approximate ratio of 3 mol of 17S/mol of 13S. Sedimentation analysis was used to verify that the 5.6S species amounted to less than 3% of the total enzyme.

Enzyme concentrations were determined from ultraviolet spectra of the protein ($\epsilon_{280}^{1\%}$ = 17.5; Taylor et al., 1974; Berman et al., 1980). Preparation of the fluorescent conjugates PBMP-AchE and DC_5MP-AchE has been described (Berman & Taylor, 1978; Epstein et al., 1979). After inhibition with the fluorescent methylphosphonofluoridate, the resultant conjugate was passed through a Sephadex G-25 column to remove unreacted label and dialyzed against 2000 volumes of buffer. Stoichiometry of labeling was ascertained from the UV spectra of the conjugates by employing the following extinction coefficients: pyrenebutyl, $\epsilon_{348} = 4.0 \times 10^4$ M^{-1} cm^{-1}; (dansylsulfonamido)pentyl, $\epsilon_{335} = 6 \times 10^3$ M^{-1} cm^{-1}. Solutions of propidium were filtered before use and concentrations determined from their absorption spectra (Berman et al., 1981).

Steady-State Fluorescence Polarization. Steady-state polarization was measured on an Aminco-Bowman Ratio II spectrofluorometer equipped with Glan-Thompson polarizers and a thermostated block to regulate cuvette temperature. Slits were set to permit a 5.5-nm spectral band-pass. Excitation and emission wavelengths for the pyrenebutyl conjugates were set at 348 and 400 nm, respectively.

Fluorescence polarization was measured by isothermal variation of viscosity with different concentrations of sucrose and by variation of temperature over the range 9–37 °C. Scatter was accounted for by simultaneous measurement of polarization from solutions containing buffer or buffer and sucrose in the absence of labeled protein.

For examination of the 11S conjugate, a 0.01 M Tris-HCl buffer, pH 8.0, containing either 0.1 N NaCl and 0.04 M $MgCl_2$ or 1 M NaCl and 0.04 M $MgCl_2$ was employed. The asymmetric (17 + 13)S forms were examined only in the Tris-HCl buffer containing 1 M NaCl and 0.04 M $MgCl_2$ to minimize aggregation. In a typical determination, the enzyme was present at concentrations between 2×10^{-7} and 5×10^{-7} M in active sites. Polarization values were observed to be independent of enzyme concentration over this range.

Fluorescence polarization is defined as

$$P = (I_{VV} - GI_{VH})/(I_{VV} + GI_{VH}) \quad (1)$$

where fluorescence intensity upon excitation with vertically polarized light is measured with the emission polarizer in the vertical (I_{VV}) and horizontal (I_{VH}) directions. The G factor, where $G = I_{HV}/I_{HH}$, serves to correct for unequal transmission by the diffraction grating of vertically and horizontally polarized light (Azumi & McGlynn, 1962).

Perrin's law (Weber, 1953) relates fluorescence polarization to the temperature (T, in kelvin) viscosity (η, in poise), fluorescence lifetime (τ, in nanoseconds), and rotational correlation time (ϕ, in nanoseconds) and predicts a linear relationship for plots of $1/P - {}^1/_3$ vs. T/η:

$$\frac{1}{P} - \frac{1}{3} = \left(\frac{1}{P_0} - \frac{1}{3}\right)\left(1 + \frac{RT\tau}{\eta V}\right) = \left(\frac{1}{P_0} - \frac{1}{3}\right)\left(1 + \frac{\tau}{\phi}\right) \quad (2)$$

The y intercept, $1/P_0 - {}^1/_3$, affords a value of the limiting polarization, a property characteristic of the fluorophore. From knowledge of the fluorescence lifetime, the rotational correlation time can be derived through τ/ϕ = slope × $(T/\eta)/(y$ intercept).

Time-Correlated Fluorescence Polarization. Fluorescence decay rates were measured by employing the single-photon counting technique on a modified Ortec spectrometer equipped with an Amperex 56 DUVP photomultiplier tube and a high-pressure (10–20 atm) hydrogen discharge lamp operating in the free running mode (Yguerabide, 1972). Samples were excited with vertically polarized light; fluorescence emission was detected with the emission polarizer in the vertical and horizontal orientations to obtain the respective intensities $I_{VV}(t)$ and $I_{VH}(t)$. Samples were maintained in a thermostated cell compartment at 20 °C. The exciting lamp delivered light pulses at a near-constant rate greater than 10 kHz. At least 20 000 counts in the peak channel were accumulated, and the

values of $I_{VV}(t)$ and $I_{VH}(t)$ were scaled to account for the different collection times required to determine these functions (Yguerabide, 1972).

The excitation and emission bands of the different fluorescent ligands were selected with the following excitation/emission filter combinations: pyrenebutyl, 350-nm interference/3-75 cutoff filters; dansyl, 7-60/7-72 cutoff; propidium, 520-nm interference/3-66 cutoff. Data were accumulated over at least 2.5 decades of intensity. The channel density for each of the fluorophores was 1.6, 0.8, and 0.2 ns/channel for pyrenebutyl, dansyl, and propidium, respectively. Anisotropy was measured with concentrations of AchE conjugates or AchE–ligand complexes between 1×10^{-6} and 2.5×10^{-5} M in active sites; scatter contributions were determined to be negligible as observed from measurements of equivalent concentrations of unlabeled native protein.

Nanosecond Polarization Spectroscopy. The explicit time dependence of the fluorescence anisotropy $A(t)$ is given by

$$A(t) = \frac{I_{VV}(t) - I_{VH}(t)}{I_{VV}(t) + 2I_{VH}(t)} = \frac{D(t)}{S(t)} \quad (3)$$

where the numerator represents the *difference* $D(t)$ and the denominator the *sum* $S(t)$ of the composite decay rates (Yguerabide et al., 1970). The sum function is analogous to the decay of the total fluorescence intensity and hence decays with a lifetime of τ. For a solution of randomly oriented macromolecules $S(t)$ depends only on the fluorescence lifetime of the fluorescence reporter group and is independent of the rotational motions of the macromolecule. Hence, it can be expressed in a manner analogous to decay of the total fluorescence intensity:

$$S(t) = S_0 e^{-t/\tau} \quad (4)$$

where S_0 denotes the intensity at zero time.

Fluorescence decay curves of the short-lived fluorophores were corrected for distortion in the early moments due to the presence of the lamp pulse by employing the method of moments as already described (Berman et al., 1980; Yguerabide, 1972). To obtain true anisotropy decay rates, the sum and difference functions in eq 3 were individually deconvoluted to obtain amplitudes and lifetimes that upon combination would afford the corrected anisotropy. For these calculations we employed the equation:

$$I(t) = \sum a_i e^{-t/\tau_i} \quad (5)$$

where the intensity, $I(t)$, is made up from functions containing one or two exponential terms. Such a procedure has been shown to resolve the experimentally observed anisotropy and permit calculation of rotational correlation times.

Anisotropy decay rates for the pyrenebutyl fluorophore were observed to be far slower than the decay of the exciting lamp pulse; hence, distortion due to the lamp pulse in the early moments following excitation could be ignored, and accordingly, we were able to resolve the time course of anisotropy by employing the Marquardt nonlinear least-squares procedure to the appropriate one- or two-exponential equation (Marquardt, 1963).

The time course of $A(t)$ is dependent on the shape and size of the macromolecule and is independent of the fluorescence lifetime of the probe under observation. This statement holds only for those cases where a single lifetime is considered (Ludescher, 1984; J. Yguerabide, unpublished results).

The anisotropy at zero time (A_0) is determined by photoselection and the directions of the absorption and emission transition moments. A maximum value of 0.4 is predicted for the situation where the transition moments are collinear. Rapid fluctuations in the orientation of the emission moments diminish the experimentally determined value. The limiting anisotropy A_0 can be related to the limiting polarization considered earlier by the relationship $A_0 = 2P_0/(3 - P_0)$.

For a rigid sphere of volume V, the decay of anisotropy is described by

$$A(t) = A_0 e^{-t/\phi} = A_0 e^{-6Dt} \quad (6)$$

where ϕ and D represent the rotational correlation time and diffusion coefficient, respectively, and are related to each other and the volume of the sphere by the relationship:

$$\phi = \eta V/kT = 1/6D \quad (7)$$

The volume, V, denotes the hydrated volume of a spherical particle, D (s^{-1}) is the rotational diffusion coefficient, η (P) is the viscosity, and k (erg deg^{-1} $molecule^{-1}$) is the Boltzmann constant.

For a rigid *oblate* ellipsoid, the calculated correlation times deviate little from each other and reflect the nearly equivalent frictional resistance encountered during motion about the major and minor axes. Hence, decay of anisotropy appears to be exponential. Rotational correlation times for a rigid *prolate* ellipsoid markedly differ with increasing axial ratio. Rotation about the long major axis occurs more easily than for an equivalent sphere, while motion about the short minor axis engenders greater frictional resistance. Consequently, as the shape of the particle deviates from spherical symmetry, the underlying rotational correlation times diverge and the decay of anisotropy will exhibit a corresponding departure from exponential behavior (Tao, 1969).

Nonexponential decay of anisotropy can also be due to intrinsic segmental flexibility. The latter phenomenon is attributed to motion of a portion of the protein structure that occurs more rapidly than and is independent of global rotation of the macromolecule. In practice, it often proves difficult to observe anisotropy decay over more than one decade of intensity, thereby providing insufficient information to justify use of an equation containing more than two exponential terms. The following equation resolves nonexponential decay into two major modes of rotational diffusion characterized by short (ϕ_S) and long (ϕ_L) correlation times and amplitudes (f_S, f_L).

$$A(t) = A_0(f_S e^{-t/\phi_S} + f_L e^{-t/\phi_L}) \quad (8)$$

RESULTS

Steady-State Fluorescence Polarization of 11S and (17 + 13)S AchE Forms. Fluorescence polarization of the covalent conjugates formed upon reaction of PBMPF with the 11S and (17 + 13)S AchE forms follows Perrin's law (Figure 1). For the 11S tetrameric form isothermal variation of viscosity yields a linear relationship between reciprocal polarization and T/η and affords a limiting polarization value of 0.29. Over a more limited range of T/η similar data were obtained by variation of temperature. Thus, no change in AchE conformation affecting rotational diffusion can be detected as a consequence of variation of these two external parameters. On the basis of an average fluorescence lifetime of 100 ns for the pyrenebutyl moiety (Berman et al., 1980), the linear Perrin relationship yields a single rotational correlation time of ~400 ns. Data from multiple determinations and separate preparations of enzyme are given in Table I. We do not observe the downward curvature described by Knopp & Weber (1969) for conjugates or pyrenebutyric acid and immunoglobulin G at high viscosities. The curvature was proposed to arise from a distribution of fluorophore probes exhibiting different mo-

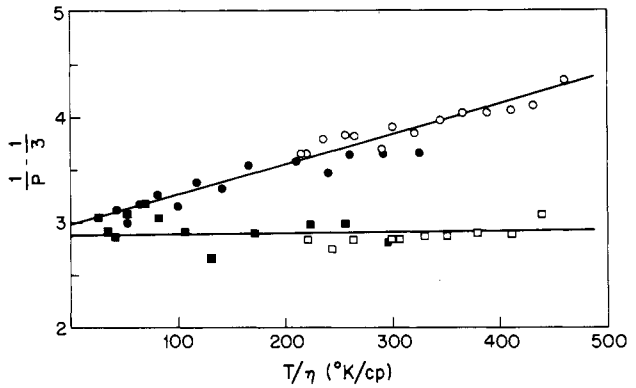

FIGURE 1: Steady-state fluorescence polarization vs. temperature/viscosity ratio for pyrenebutyl methylphosphono conjugates of acetylcholinesterase molecular forms. Polarization data are presented as $(1/P - 1/3)$ vs. T/η, where P is polarization, T is temperature (K), and η is viscosity (cP). Data were obtained by isothermal variation of viscosity at 23 °C upon addition of sucrose (●, ■) and thermal variation at different temperatures in the range 8–40 °C (○, □). Presented are data obtained by thermal and isothermal variation of viscosity for PBMP conjugates of the 11S form (○, ●) and the (13 + 17)S forms (□, ■). Data for both the lytic 11S and tailed (13 + 17)S molecular forms approach common values of approximately 2.8–3.0 at the y intercept, corresponding to limiting polarizations of 0.29 ± 0.01 and 0.32 ± 0.02, respectively. With a lifetime of 100 ns for the conjugated pyrenebutyl moiety, the rotational correlation times are estimated to be 400 ns for the 11S form and greater than 1100 ns for the asymmetric tailed forms.

Table I: Polarization Values from Steady-State Studies of Pyrenebutyl Methylphosphono Conjugates of Acetylcholinesterase Molecular Forms

molecular form and method	P_0	slope [(K/P)$^{-1}$]	ϕ (ns)
11S			
isothermal (3)[a]	0.29 ± 0.01	(2.37 ± 0.25) × 10^{-5}	419 ± 50
thermal (2)	0.29 ± 0.01	(2.68 ± 0.38) × 10^{-5}	364 ± 63
(13 + 17)S			
isothermal (4)	0.32 ± 0.02	(3.5 ± 5.5) × 10^{-6}	>1100
thermal (3)	0.32 ± 0.02	(1.4 ± 5.9) × 10^{-6}	>1100
trypsin-treated (17 + 13)S[b]			
isothermal (1)	0.28	2.38 × 10^{-5}	466

[a] Mean ± standard error. The numbers of determinations are indicated in parentheses. The rotational correlation times are calculated from eq 2 employing a fluorescence lifetime of 100 ns, a value that represents the weighted average of the two lifetimes characteristic of PBMP-AchE determined by time-correlated nanosecond spectroscopy (Berman et al., 1980). Perrin plots for the (17 + 13)S conjugates yielded shallow slopes, some of which were negative. The negative values were considered in the calculation of the mean. This accounts for the standard error being larger than the mean, which falls close to the zero value. [b] Determined following treatment of (17 + 13)S AchE with 5.0 μg/mL trypsin for 30 min at 37 °C (see text for details).

lecular motion. PBMPF has been shown to label only the active site serine on each subunit.

Fluorescence polarization of PBMPF conjugates of the (17 + 13)S elongated forms of AchE shows slopes that do not differ from zero upon variation of T/η over the temperature range 9–37 °C and isothermal variation of viscosity with different quantities of sucrose. Limiting polarization values P_0 are essentially identical with those obtained with the 11S enzyme, as would be anticipated if the same active center was being modified by the fluorophore (Table I). When measurements are averaged over four isothermal variations of viscosity, an average rotational correlation time of 1100 ns is obtained (Table I). Should the rotational correlation time have been less than 1100 ns, it would have been detectable as a nonzero slope in the multiple measurements. Temperature-dependent changes in polarization are reversible, and identical polarization profiles are obtained upon heating or cooling of the sample over the temperature range 9–37 °C.

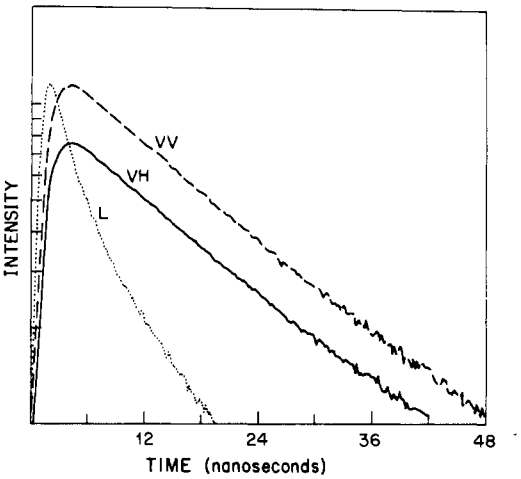

FIGURE 2: Decay of polarized components for complexes of acetylcholinesterase and propidium. Propidium and acetylcholinesterase (15 μM in subunit sites) were present in a stoichiometric ratio of 0.8/1. Horizontal and vertical intensities are denoted as VH and VV, respectively, and the shape of the lamp profile is denoted as L. Experimental conditions are described under Experimental Procedures.

In a separate experiment the (17 + 13)S enzyme, which showed a zero slope upon thermal variation of T/η, was treated with trypsin (5 μg/mL for 30 min at 37 °C) followed by 5 μg/mL soybean trypsin inhibitor. This procedure is identical with that employed to release 11S enzyme from the crude particulate fraction (Taylor et al., 1974). When the isolated (17 + 13)S enzyme is treated with trypsin, the predominant species obtained is the 11S species. Fluorescence polarization measurements following treatment with trypsin yield values of P_0 and ϕ essentially identical with those obtained for the isolated 11S species (Table I).

Time-Correlated Fluorescence Polarization. Anisotropy decay rates for complexes of 11S AchE with propidium reversibly bound at the peripheral site and for PBMP-AchE and DC_5MP-AchE covalently conjugated at the active center were determined by measuring the time dependence of $I_{VV}(t)$ and $I_{VH}(t)$. Figure 2 illustrates traces obtained for decay of the individual polarized components characteristic of complexes of propidium and AchE. The time dependences of the anisotropy calculated from these data and similar data for the PBMP and DC_5MP conjugates of AchE are shown in Figure 3. For the peripheral site probe the semilogarithmic plots of $A(t)$ vs. time appear linear over a 40-ns range of measurement and are described adequately by a single exponential function. Values for A_0 and the rotational correlation time ϕ for the propidium complex are calculated to be 0.34 and ~150 ns, respectively. The results obtained appear to be independent of ionic strength since similar values are obtained in buffer containing 0.1 N NaCl and 0.04 M $MgCl_2$ (not shown). The short lifetime of propidium (6 ns) yields only a truncated decay curve that likely precludes detection of a global rotational correlation time.

The covalent conjugate of AchE containing the (dansylsulfonamido)pentyl fluorophore situated at the active center displays only a slight departure from an exponential behavior for decay of polarization. The data can be essentially described by a single exponential function for which A_0 and the rotational correlation time are calculated to be 0.31 and 322 ns, respectively. The value for A_0 appears to be characteristic of the dansyl fluorophore and is in agreement with that obtained

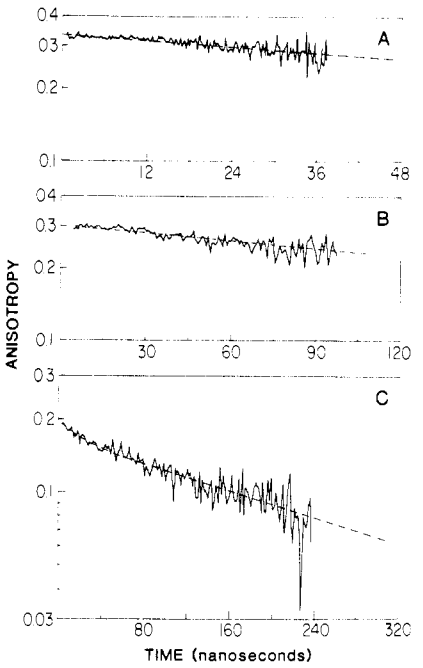

FIGURE 3: Anisotropy decay for three fluorophores associated with acetylcholinesterase. Panel A: Complex of acetylcholinesterase and propidium. The dashed line is calculated from a single exponential function (eq 6) in which the rotational correlation time is predicted to be 150 ns. Panel B: [(Dansylsulfonamido)pentyl methylphosphono]acetylcholinesterase. The dashed line is calculated from a single exponential function (eq 6) in which the rotational correlation time is predicted to be 322 ns. Panel C: (Pyrenebutyl methylphosphono)acetylcholinesterase. The dashed line is calculated from a two-exponential function (eq 8) in which the two rotational correlation times of 28 and 320 ns are present in amplitudes of 0.13 and 0.87, respectively.

for a number of other protein conjugates in which the dansyl moiety is immobilized (Hanson et al., 1981; Holowka & Cathou, 1976).

Decay of anisotropy measured for PBMP-AchE exhibits a significant deviation from exponential behavior and is more adequately described over the 300-ns duration by a function containing two exponential terms (eq 8). Resolution of the calculated anisotropy derived from the individual polarized components, employing Marquardt's nonlinear least-squares treatment (Marquardt, 1963), affords a component of low amplitude (f_S = 0.13) characterized by a correlation time of 28 ns and a component of higher amplitude (f_L = 0.87) characterized by a long correlation time of 320 ns. In an alternative treatment, $A(t)$ was calculated as the quotient of $D(t)$ and $S(t)$ (eq 2), where each of these functions was resolved by employing the method of moments to afford amplitudes and decay rates for the sum function [$S(t)$: a_1, 6428 (31%); a_2, 14529 (69%); τ_1, 44.8 ns; τ_2, 114 ns] and the difference function [$D(t)$: a_1, 1343 (33%); a_2, 2770 (67%); τ_1, 22.6 ns; τ_2, 80 ns]. Marquardt analysis of $A(t)$ calculated as the quotient $D(t)/S(t)$ (eq 2) affords amplitudes and correlation times for the short (f_S = 0.16; ϕ_S = 16.5 ns) and long (f_L = 0.84; ϕ_L = 309 ns) components that are in reasonable agreement with the results obtained from a method of moments calculation of the individual components without resolving $S(t)$ and $D(t)$.

The lifetimes, A_0 values, and calculated rotational correlation times for the reversible complex of 11S AchE with propidium and for the covalent active center conjugates are summarized in Table II. It is noted that decay of fluorescence anisotropy obtained with three independent fluorescence probes situated at two topographically distinct sites on AchE indicates

Table II: Anisotropy of Various Complexes and Conjugates of 11S Acetylcholinesterase[a]

enzyme complexes and conjugates	τ (ns)	A_0	ϕ_L (ns)	f_L	ϕ_S (ns)	f_S
propidium/AchE	6	0.34	150	1.00		
DC_5MP-AchE	16	0.31	322	1.00		
PBMP-AchE[c]	100[b]	0.20	320	0.87	28	0.13
PBMP-AchE[d]	100	0.20	310	0.84	16	0.16

[a] Column headings are lifetime (τ), initial limiting anistropy (A_0), rotational correlation time (ϕ), and amplitude (f); subscripts S and L denote short and long components. [b] Fluorescence emission was characterized by two lifetimes (Berman et al., 1980). These values are the average values calculated from $\langle\tau\rangle = (a_1\tau_1 + a_2\tau_2)/(a_1 + a_2)$. [c] Calculated from anisotropy obtained from individual polarized components [$I_{VV}(t)$. $I_{VH}(t)$]. [d] Calculated from anisotropy resolved according to difference and sum functions, eq 3.

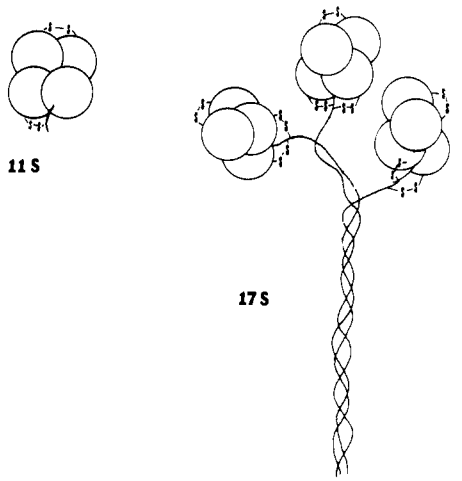

FIGURE 4: Structures of the asymmetric (17S) and the lytic (11S) species of acetylcholinesterase. The asymmetric forms are arranged as tetramers of catalytic subunits disulfide-linked to a tail unit of triple-helical conformation. The generalized structure of the 17S species is illustrated. The 13S species differs from the 17S species by the absence of one of the tetramers. The tail unit is collagen-like at the end distal to the catalytic subunits. The *Torpedo* enzyme differs from the corresponding enzyme species from *Electrophorus* by the presence of a second structural subunit present in low abundance (not shown). The 11S species is formed by proteolysis of the asymmetric species [see Massoulié & Bon (1982) and Lee et al. (1982a,b) for details].

that the predominant mode of depolarization is characterized by correlation times that fall in the range of 150–320 ns.

Discussion

Steady-State Fluorescence Polarization of the (17 + 13)S and 11S Species. The 13S and 17S species of acetylcholinesterase are characterized by two and three sets of tetramers of catalytic subunits, respectively, that are disulfide-linked to a triple-helical collagen-containing tail unit 500 Å in length [cf. Massoulié & Bon (1982)] (Figure 4). A second, noncollagenous structural subunit proximal to the catalytic subunits is also present in low abundance in the *Torpedo* species (Lee et al., 1982a). Treatment with trypsin removes the structural subunits, giving rise to the 11S form (Figure 4). Electron microscopy of these asymmetric molecular forms of AchE reveals that each strand of the triple-helical tail may connect with a single tetrameric assembly of catalytic subunits (Cartaud et al., 1975). Both the 13S and 17S species share this common structure and are believed to differ only in the absence of one set of tetramers in the 13S species (Lwebuga-Mukasa et al., 1976; Reiger et al., 1976; Lee et al., 1982a). Hence, the restrictions imposed by the tail unit on molecular motion of the catalytic subunits are expected to be very similar

in both the 13S and 17S species.

Restricted rotational motion of the (17 + 13)S forms may arise through either intrinsic rigidity in the tail unit or noncovalent association of the tethered individual tetramers. In the latter case, the tail unit may be flexible, but association of proximal tetramers would hinder rotational diffusion. Conversely, when the (17 + 13)S and 11S forms are compared, minimal restriction of rotational motion would reflect the flexibility of a hinge-like region on the tail unit proximal to the catalytic subunits and the lack of association of the tail-linked tetramers. The increase in rotational correlation times from 400 ns seen in the 11S species to greater than 1100 ns observed for the (17 + 13)S species (Table I) indicates a marked hindrance of motion of the tetramer of catalytic subunits imposed by the tail unit. That this motion is attributable to association of the globular domains with the tail unit is supported by the observation that proteolytic digestion of the tail unit serves to relieve the motional restrictions and, in turn, diminish the rotational correlation time. Spherical, rigid molecules of masses of 1.1×10^6 (17S) and 8.1×10^5 (13S) daltons would be predicted to show rotational correlation times in the neighborhood of 325–440 ns (see discussion below). Dimensional asymmetry of the elongated species has been well documented in previous hydrodynamic studies (Lee et al., 1982a,b) and accounts for the rotational correlation times extending into the microsecond range.

The *Torpedo* enzyme possesses collagenous (40K) and noncollagenous (100K) subunits; the latter is not found in AchE from *Electrophorus* (Rosenberry & Mays, 1981). Initial measurements of steady-state polarization as a function of T/η with the (18 + 14)S enzyme from *Electrophorus* reveal, as seen for the enzyme from *Torpedo*, a slope indistinguishable from zero (H. A. Berman, unpublished observations). Hence, it is likely that the restrictions imposed by the tail unit on motional freedom of the catalytic subunits are also manifest in the tail-containing *Electrophorus* species and represent a structural feature common to the collagen tail-containing asymmetric forms of AchE.

Analysis of Time-Correlated Anisotropy Decay for 11S Acetylcholinesterase. Time-correlated anisotropy decay for fluorophores associated with the 11S acetylcholinesterase reveals more than a single rotational correlation time. For the propidium–AchE complex anisotropy decay occurs with a single rotational correlation time of approximately 150 ns, whereas the covalent active center (dansylsulfonamido)pentyl and pyrenebutyl methylphosphono conjugates afford substantially longer rotational correlation times in the range of 320 ns. The pyrenebutyl methylphosphono conjugate allows estimation of the decay kinetics to times exceeding 200 ns and reveals two clearly resolved components of rotational relaxation. The shorter one of 16–28 ns represents less than 15% of the total amplitude, while the decay time of the predominant longer lived component of 320 ns is in excellent agreement with that observed with the dansyl conjugate. For the covalent (dansylsulfonamido)pentyl and pyrenebutyl adducts, the observed correlation times are far longer than that expected if the fluorophores exhibited torsional motions about the bond of conjugation. Hence, the fluorophores appear to be rigidly affixed to the enzyme surface.

The anisotropy decay of the 11S AchE form is interpreted in relation to two limiting models. The first model considers the 11S molecular form to behave as a *rigid* particle of either spherical or ellipsoidal symmetry. The second model considers the enzyme to exhibit segmental motion independent of the global rotation of the macromolecule. In the evaluation of both models, experimental data are compared with correlation times expected for rigid spheres and ellipsoids of different axial ratios calculated from existing hydrodynamic data.

Rotational Correlation Times Predicted from Hydrodynamic Data of Spherical and Ellipsoidal Particles. The 11S form of acetylcholinesterase has a molecular weight of 330000 as determined by sedimentation equilibrium. On the basis of this molecular weight, a partial specific volume $\bar{V}$ of 0.716 cm^3/g estimated from the amino acid and carbohydrate compositions (Taylor et al., 1974), and a typical estimate of hydration volume h (0.23 cm^3/g), a molecular volume V of 0.52×10^{-18} cm^3 is calculated from the equation:

$$V = M_r(\bar{V} + h)/N \quad (9)$$

The rotational correlation time for a rigid sphere of this molecular volume is calculated to be 130 ns. The observed Stokes radius (76 Å) and calculated frictional coefficient ($f/f_0 = 1.65$) reveal that the 11S form of AchE exhibits substantial dimensional asymmetry, abnormal hydration, or both. The frictional coefficient may be compared with values of 1.1–1.25 expected for globular proteins that approach spherical dimensions.

If dimensional asymmetry alone is responsible for the hydrodynamic properties, then a frictional coefficient of 1.65 for prolate and oblate ellipsoids would be consistent with axial ratios of 11/1 and 10/1, respectively (Tao, 1969; Cantor & Schimmel, 1980). Axial ratios of this magnitude yield for oblate and prolate ellipsoids rotational correlation times at least 5 times that of a rigid sphere (Tao, 1969). As estimated by Kuntz & Kauzmann (1974), the influence of hydration on hydrodynamic behavior of proteins would reduce the asymmetry contribution of f/f_0 to values of 1.35–1.40, yielding in turn axial ratios between 4 and 7 for the oblate and prolate particles. Calculated rotational correlation times in these cases fall to 3–4-fold greater than that of a rigid sphere of equal volume.

The correlation times we observe fall under those values (>390 ns) predicted for rotational diffusion about the major axes for these ellipsoids of revolution. Although the presence of long correlation times could go undetected for the shorter lived probes, the data obtained with the pyrenebutyl ligand indicate that the presence of a long correlation time would be of small amplitude. To distinguish whether a rigid ellipsoid or a flexible structure possessing segmental motion best fits the anisotropy data for the three fluorescent adducts, we have employed the analyses of normalized anisotropy introduced by Yguerabide et al. (1970) [cf. Yguerabide (1972)].

Normalized Anisotropy Analyses. Rotational depolarization for the case in which the fluorescent probes are distributed so that their emission transition moments are randomly oriented with respect to the major axis of an ellipsoidal particle is described by an equation containing three exponential terms (eq A1). By use of this equation and the formalism described in the Appendix, normalized anisotropy for a series of oblate and prolate ellipsoidal particles of different axial ratios can be calculated and compared with the experimental data. In this method $A(t)/A_0$ is plotted on a logarithmic scale vs. t/ϕ, where t is time and ϕ is the rotational correlation time for a rigid sphere.

The results of these analyses are presented in Figure 5, in which the experimental data of the propidium–AchE complex and those prototypic of the active center ligands ($\phi = 322$ ns) are compared with anisotropy decay calculated for prolate (panel A) and oblate (panel B) ellipsoids of different axial ratios. Two features of these comparisons are noteworthy. The first finding is that the data for propidium are compatible with

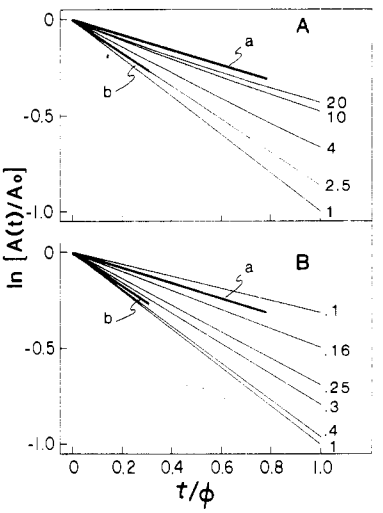

FIGURE 5: Comparison of observed and calculated normalized anisotropy plots. The heavy lines are the normalized emission anisotropy data for [(dansylsulfonamido)pentyl methylphosphono]acetylcholinesterase (curves a) and AchE complexed with propidium (curves b). These curves were calculated by using ϕ = 130 ns and A_0 = 0.31 (curves a) and A_0 = 0.34 (curves b). The light lines are normalized emission anisotropy curves calculated for rigid prolate (panel A) and oblate (panel B) ellipsoids ranging in axial ratio from 1 to 20 and 1 to 10, respectively. The anisotropy decay for the slow component of the pyrenebutyl methylphosphono conjugate is virtually identical with that of the (dansylsulfonamido)pentyl conjugate but would extend to a ratio of ~2 on the time axis.

rotational diffusion of a rigid prolate particle of axial ratio 2.5/1 or of a rigid oblate particle of axial ratio 1/3. The short fluorescence lifetime precludes our distinguishing these alternatives. The results obtained for the covalent active center conjugates, in contrast, are incompatible with rotational depolarization of a rigid prolate particle of axial ratio as great as or greater than 20/1. The data appear to coincide with rotational depolarization of a rigid oblate ellipsoid of axial ratio approximately 1/8. Hence, on the basis of comparison with rigid ellipsoidal particles the results obtained with propidium require dimensional asymmetry that is markedly distinct from that indicated from study of the active center conjugates. Although propidium has been shown to influence active center conformation through binding to the peripheral anionic site (Epstein et al., 1979), a shape change of this magnitude for a tetrameric molecule seems unlikely.

On the basis of fluorescence energy transfer studies, the site of propidium binding is some 25 Å removed from the active center (Berman et al., 1980), and thus it seems likely that the propidium site on each subunit is located on a domain separate from the active center. Should segmental motion be manifest, then ligands bound on these separate domains may be expected to exhibit rotational correlation times that are divergent from as well as faster than that of the macromolecule. The short lifetime of propidium precludes detection of a global rotation, and hence the data do not allow a clear resolution of this point.

A second finding favoring segmental motion is the observation of two distinct correlation times for (pyrenebutyl methylphosphono)acetylcholinesterase. The shorter correlation time greatly exceeds that predicted for free rotation about the bonds of the conjugated fluorophore and likely corresponds with motion of a larger segment of the individual subunits. Employing the relationship $\cos^2\theta = (2f_L + 1)/3$ (Yguerabide et al., 1970), we calculate that the faster depolarization reflects motion of the active center domain over an angle of 17–18°. Such an angular deflection would correspond to the motion of a 20 000–30 000-dalton segment.

Thus, the data point to the acetylcholinesterase tetramer exhibiting segmental motion, the very existence of which precludes our obtaining estimates of the global rotation and hence shape of the macromolecule. The depolarization studies nevertheless point to dimensional asymmetry inherent in the tetrameric 11S species, as previously inferred from gel diffusion studies (Taylor et al., 1974). For a multisubunit protein, however, the widely used model of an ellipsoidal particle to approximate dimensional asymmetry may not be appropriate. A tetrameric arrangement of nondeformable spherical subunits, for example, whether grouped in tetrahedral or square-planar geometries will give rise to frictional coefficients in the range 1.6–1.8 (Bloomfield et al., 1967; Cantor & Schimmel, 1980) without the necessity of assuming an ellipsoidal shape. The experimental correlation times we observe (150 ns for the bound propidium and 320 ns for the active center conjugates) reflect motion of discrete segments of the macromolecule. Since the correlation times are not compatible with the rigid-particle models examined, depolarization occurs more rapidly than predicted for global rotation of a rigid tetrameric molecule with frictional coefficient of 1.65.

APPENDIX

Fluorescence Depolarization and Rotational Brownian Motion of Asymmetric Molecules. Anisotropy decay for a rigid symmetric molecule is described by an exponential equation (6) (see Experimental Procedures). For an asymmetric molecule, when rotational diffusion about its principal axes differs considerably, the isotropic constraints break down and are replaced by an anisotropic description containing five exponential terms (Chuang & Eisenthal, 1972; Ehrenberg & Rigler, 1972; Belford et al., 1972). For a collection of identical sites in which the fluorophore emission transition moment is randomly oriented with respect to the major axis of an ellipsoid the equation describing anisotropy decay simplifies to (Ehrenberg & Rigler, 1972)

$$A(t) = (A_0/5)[\exp(-t/\phi_1) + 2\exp(-t/\phi_2) + 2\exp(-t/\phi_3)] \quad \text{(A1)}$$

where ϕ_1, ϕ_2, and ϕ_3 denote rotational correlation times and are related to the rotational diffusion coefficients about the major ($D_\parallel$) and minor ($D_\perp$) axes according to

$$\phi_1 = 1/6D_\perp$$
$$\phi_2 = 1/(5D_\perp + D_\parallel) \quad \text{(A2)}$$
$$\phi_3 = 1/(2D_\perp + 4D_\parallel)$$

The diffusion coefficients contain the structural information pertaining to the macromolecule and can be arranged into a set of equations dependent on the axial ratio (γ) of the ellipsoid and the diffusion coefficient of a sphere of equivalent volume (D).

$$\frac{D_\perp}{D} = \frac{3}{2}\frac{\gamma[(2\gamma^2 - 1)\beta - \gamma]}{\gamma^4 - 1} \quad \text{(A3a)}$$

$$\frac{D_\parallel}{D} = \frac{3}{2}\frac{\gamma(\gamma - \beta)}{\gamma^2 - 1} \quad \text{(A3b)}$$

For a prolate ellipsoid

$$\beta = \frac{1}{(\gamma^2 - 1)^{1/2}} \ln[\gamma + (\gamma^2 - 1)^{1/2}]$$

and for an oblate ellipsoid

$$\beta = \frac{1}{(1 - \gamma^2)^{1/2}} \tan^{-1}\frac{(1 - \gamma^2)^{1/2}}{\gamma}$$

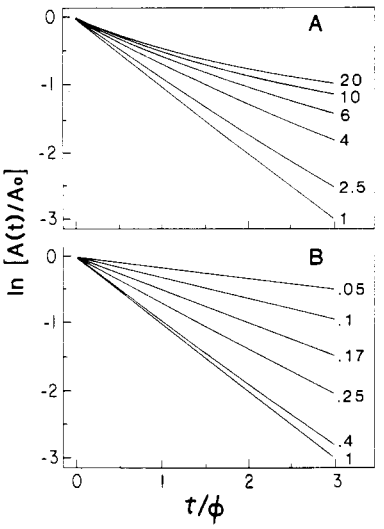

FIGURE 6: Time dependence of the normalized anisotropy for rigid ellipsoids ranging in axial ratio from 1 to 20. Panel A presents the normalized anisotropy curves calculated for prolate particles, and panel B presents similar calculations for oblate particles. In the calculations, the fluorophore is assumed to be randomly oriented with respect to the ellipsoid axes.

These equations can be employed to normalize the anisotropy (eq A1) relative to that expected for a rigid sphere of volume equal to that of the ellipsoid.

$$A(t) = (A_0/5)[\exp(-t/\phi)\Omega_1 + 2\exp(-t/\phi)\Omega_2 + 2\exp(-t/\phi)\Omega_3] \quad \text{(A4)}$$

In this formulation the exponential terms are functions of ϕ and Ω, a series of constants dependent on the ratio of diffusion coefficients (eq A5).

$$\Omega_1 = D_\perp/D$$
$$\Omega_2 = (5D_\perp + D_\parallel)/6D \quad \text{(A5)}$$
$$\Omega_3 = (2D_\perp + 4D_\parallel)/6D$$

For rigid ellipsoids and the case of random orientation of the emission transition moments, plots of ln $[A(t)/A_0]$ vs. t/ϕ are dependent solely on the axial ratio, while the volume V chosen for calculation of ϕ merely compresses or expands the time scale. The family of curves in Figure 6 represent a graphical description of eq A5 for prolate (panel A) and oblate (panel B) particles. When normalized anisotropy is calculated to times approaching 3ϕ, increasing curvature with increasing asymmetry of prolate particles is readily apparent. The normalized anisotropy for oblate ellipsoids, in contrast, shows a distinctive pattern of only slight deviation from exponential behavior (Tao, 1969). Visual comparison of these curves with the experimental data permits estimation of γ and V, thereby affording measures of the size and shape of the macromolecule.

Registry No. AchE, 9000-81-1.

REFERENCES

Azumi, T., & McGlynn, S. P. (1962) *J. Chem. Phys. 37*, 2413–2420.

Belford, G. G., Belford, R. L., & Weber, G. (1972) *Proc. Natl. Acad. Sci. U.S.A. 69*, 1392–1393.

Berman, H. A., & Taylor, P. (1978) *Biochemistry 17*, 1704–1713.

Berman, H. A., Yguerabide, J., & Taylor, P. (1980) *Biochemistry 19*, 2226–2235.

Berman, H. A., Becktel, W., & Taylor, P. (1981) *Biochemistry 20*, 4803–4810.

Bloomfield, V., Dalton, W. O., & Van Holde, K. E. (1967) *Biopolymers 5*, 135–148.

Bon, S., & Massoulié, J. (1980) *Proc. Natl. Acad. Sci. U.S.A. 77*, 4464–4468.

Cantor, C. R., & Schimmel, P. R. (1980) *Biophysical Chemistry*, Part II, Chapter 10, W. H. Freeman, San Francisco.

Cartaud, J., Reiger, F., Bon, S., & Massoulié, J. (1975) *Brain Res. 88*, 127–130.

Chuang, T. J., & Eisenthal, K. B. (1972) *J. Chem. Phys. 57*, 5094–5097.

Ehrenberg, M., & Rigler, M. (1972) *Chem. Phys. Lett. 14*, 539–544.

Epstein, D., Berman, H. A., & Taylor, P. (1979) *Biochemistry 18*, 4749–4754.

Hanson, D. C., Yguerabide, J., & Schumaker, V. N. (1981) *Biochemistry 20*, 6842–6852.

Holowka, D. A., & Cathou, R. E. (1976) *Biochemistry 15*, 3379–3390.

Knopp, J., & Weber, G. (1969) *J. Biol. Chem. 244*, 6309–6315.

Kuntz, I. D., Jr., & Kauzmann, W. (1974) *Adv. Protein Chem. 28*, 239–345.

Lee, S. L., & Taylor, P. (1982) *J. Biol. Chem. 257*, 12292–12301.

Lee, S. L., Heinemann, S., & Taylor, P. (1982a) *J. Biol. Chem. 257*, 12283–12291.

Lee, S. L., Camp, S. J., & Taylor, P. (1982b) *J. Biol. Chem. 257*, 12302–12309.

Ludescher, R. D. (1984) *Biophys. J. 45*, 379a (Abstr.).

Lwebuga-Mukasa, J., Lappi, S., & Taylor, P. (1976) *Biochemistry 15*, 1425–1434.

Marquardt, D. W. (1963) *J. Soc. Ind. Appl. Math. 2*, 431–441.

Massoulié, J., & Bon, S. (1982) *Annu. Rev. Neurosci.* 5, 57–106.

Mooser, G., & Sigman, D. S. (1974) *Biochemistry 13*, 2299–2307.

Pattison, S., & Bernhard, S. (1978) *Proc. Natl. Acad. Sci. U.S.A. 75*, 3613–3617.

Reiger, F., Bon, S., Massoulié, J., Cartaud, J., Picard, B., & Benda, P. (1976) *Eur. J. Biochem. 68*, 513–521.

Rosenberry, T. L., & Mays, C. (1981) *Biochemistry 20*, 2810–2817.

Tao, T. (1969) *Biopolymers 8*, 609–632.

Taylor, P., & Lappi, S. (1975) *Biochemistry 14*, 1989–1997.

Taylor, P., Jones, J. W., & Jacobs, N. M. (1974) *Mol. Pharmacol. 10*, 78–92.

Viratelle, O. M., & Bernhard, S. A. (1980) *Biochemistry 19*, 4999–5007.

Weber, G. (1953) *Adv. Protein Chem. 8*, 415–459.

Yguerabide, J. (1972) *Methods Enzymol. 26*, 498–578.

Yguerabide, J., Epstein, H. F., & Stryer, L. (1970) *J. Mol. Biol. 51*, 573–590.